Experimental tests of Bell's inequalities based on space-time and spin variables

T. B. Pittman, Y. H. Shih, A. V. Sergienko, and M. H. Rubin
Department of Physics, University of Maryland Baltimore County, Baltimore, Maryland 21228
(Received 18 November 1994)

Coincidence detections are measured between the output ports of a beam splitter whose input is an orthogonally polarized two-photon state produced in type-II spontaneous parametric down-conversion. When the delays between the two optical paths leading to each detector are varied by two spatially separated Pockel cells, a two-photon interference effect is seen that highlights a simultaneous entanglement in both spin and space-time variables. In contrast to all previous experimental tests of Bell's inequalities, which have utilized states entangled with respect to only one type of observable, the double entanglement realized here allows the demonstration of two different types of Bell inequality violations in one experimental setup.

PACS number(s): 03.65.Bz, 42.50.Dv

Experimental tests of Bell's inequalities have provided valuable information in support of certain quantum-mechanical predictions over those of hidden-variable theories obeying the notions of locality and reality suggested in the gedanken experiment of Einstein, Podolsky, and Rosen (EPR) [1]. In these experiments, the correlations between the observables of two spatially separated but entangled particles are studied and found to be in agreement with quantum theory while violating inequalities imposed by Bell [2] on local hidden-variable models. Following Bohm's modification of the EPR argument [3], the earliest tests involved using atomic cascade decays [4–8], and later spontaneous parametric down-conversion (SPDC) [9,10], to create a superposition of discrete two-photon spin states. In general, these experiments used spatially separated polarizers in coincidence detection schemes to demonstrate violations of Bell's inequalities based on the polarization correlations of the emitted photon pairs.

More recently, however, there has been substantial activity concerning Bell's inequalities based on nonspin observables [11,12]. In particular, there have been many proposals and experiments based on continuous variables such as phase and momentum [13,14], or energy and time [15–17]. By separating the photons of a correlated pair and measuring coincidence detections as a function of some phase difference imposed between them, these experiments observe effects that cannot be explained by any classical model. Furthermore, certain measurements have exceeded Bell's limits and require any realistic interpretation of the quantum-mechanical predictions to be nonlocal.

Therefore, we can divide the above experiments into two classes that are quite different in terms of which type of observable (i.e., spin or nonspin) is being considered. Nonetheless, a common feature of all these experiments is their reliance on two-photon states that are entangled with respect to only one type of observable. It is possible, however, to have two-photon states that are entangled with respect to more than one type of observable. For example, in this paper we wish to report an experiment that realizes a two-photon state that is simultaneously entangled in both spin and space-time variables. Consequently, we are able to demonstrate two different types of Bell inequality violations in a single experimental setup.

The state originates with the photon pair produced in the spontaneous parametric down-conversion process, in which an intense laser pump beam is incident on a birefringent crystal. The nonlinear optical interactions allow the pump to generate correlated pairs of photons subject to the phase-matching conditions

$$\omega_1+\omega_2=\omega_p, \quad \mathbf{k}_1+\mathbf{k}_2=\mathbf{k}_p \ , \tag{1}$$

which link the frequencies and wave number vectors of the signal (subscript 1), the idler (subscript 2), and the pump photons inside the crystal [18]. Whereas the vast majority of previous SPDC experiments have relied on type-I phase matching, in which the down-converted photons have parallel polarizations, the spin entanglement of necessity in this experiment stems from the type-II phase-matching process in which the photons of the output pair are orthogonally polarized in the ordinary- (o) and extraordinary- (e) ray planes of the down-conversion crystal. The pair is then sent collinearly through a series of quartz plates and enters a single port of a beam splitter. A Pockel cell, followed by a photon-counting detector package, is placed in each of the output paths of the beam splitter. Due to the birefringence of the quartz plates and Pockel's cells, there are essentially two optical paths leading to each detector and the coincidence measurements realize a two-photon state of the form

$$\Psi_{\mathrm{EPR}}=A(X_1,X_2)-A(Y_1,Y_2) \ , \tag{2}$$

where X_i and Y_i, $i=1,2$, correspond to the fast and the slow axes of the birefringent materials. $A(X_1,X_2)$ and $A(Y_1,Y_2)$ therefore respectively describe the cases in which both photons take the fast paths or both photons take the slow paths to the detectors, and it follows that Eq. (2) indicates a state that is simultaneously entangled in both spin and space-time variables. The space-time

part is very similar to that of the "Franson-type" experiments [15] in which each member of the photon pair enters its own two-path (short or long) interferometer. What is different here, however, is that the space-time EPR state is realized by a cancellation of probability amplitudes rather than a short coincidence time window [17,19,20]. This cancellation is a direct consequence of the state's polarization entanglement and the resulting double entanglement leads to the demonstration of Bell inequality violations based on either spin or space-time variables.

This cancellation effect was first observed in an experiment that varied the time delay between the two terms of Eq. (2) by means of a single Pockel cell placed in front of the beam splitter in a similar setup [21]. A two-photon quantum interference pattern was clearly demonstrated, but the use of the single Pockel cell made any discussions of nonlocality or tests of Bell's inequalities based on space-time variables irrelevant. Here the delay is controlled by using two spatially separated Pockel cells after the beam splitter so that we may test Bell's inequality based on space-time variables. Furthermore, the use of rotating polarization analyzers following each Pockel cell allows us to test Bell's inequalities based on polarization.

A schematic of the experimental setup is shown in Fig. 1. An $8\times8\times(0.56\pm0.05)$ mm^3 β-BaB_2O_4 (BBO) nonlinear crystal that is cut at a type-II phase-matching angle generates pairs of orthogonally polarized, 702.2 nm in wavelength, signal and idler photons when it is pumped by the 351.1-nm line of an argon-ion laser. The collinear pair is then separated from the pump by a uv grade fused silica quartz prism and travels through 2.4 mm of quartz. The quartz is carefully aligned so that its *o*-ray polarization plane is parallel to the *e*-ray polarization plane of the BBO crystal. Since quartz is a positive crystal and BBO is negative, the optical delay created between the signal and idler photons inside the BBO crystal is exactly reversed in the quartz plates. As reflected by the $DL/2$ term in Eq. (8), this compensation results in the complete overlap of the ordinary and extraordinary space-time parts of the two-photon wave function, which was demonstrated in anticorrelation measurements presented elsewhere [22]. Eleven more quartz plates whose fast axes are aligned at 45° relative to the *o*-ray polarization plane of the BBO crystal follow the compensation quartz. Each of the 11 plates is (1 ± 0.1) mm thick, resulting in an optical path delay of about 99 μm between the fast and slow axes "channels" at wavelengths around 700 nm. On the other hand, the coherence length of each of the down-converted fields is only about 40 μm. The photon

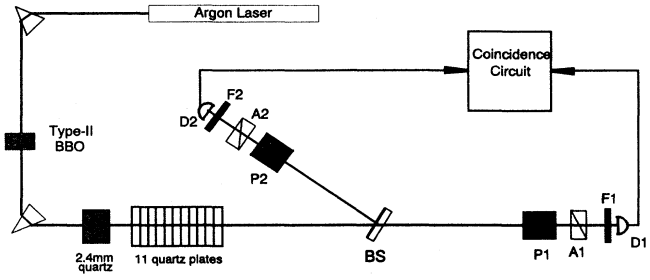

FIG. 1. Schematic of the experiment.

pair then enters a single input port of a polarization independent 50%-50% beam splitter. A Pockel cell, whose fast and slow axes are aligned to match the 11 quartz plates, is placed in each of the two output paths of the beam splitter (P1 and P2). Following each Pockel cell is a detection package comprised of a Glan Thompson linear polarization analyzer (A1 and A2), a 9-nm full width at half maximum spectral filter centered at 702.2 nm (F1 and F2), and a dry-ice-cooled avalanche photodiode operating in the Geiger mode (D1 and D2). For the space-time measurements, the Glan Thompson analyzers are oriented at 0° relative to the *o*-ray plane of the BBO crystal and the difference in the two optical paths leading to either detector is realized by changing the applied voltage on its corresponding Pockel cell. Finally, the output pulses of each detector are sent to a coincidence counting circuit with a 1.8-ns time window. Since the detector packages are separated by about 2 m, we have spacelike separated detection events.

What follows is a simplified explanation of the coincidence counting rate that highlights the nature of the simultaneous spin and space-time entanglement of the two-photon state. We start with the standard description of the two-photon state produced in type-II SPDC [18]

$$|\psi\rangle=\int d\omega_1\delta(\omega_1+\omega_2-\omega_p)\psi(k_1+k_2-k_p)\times a_0^\dagger[\omega_1(k_1)]a_e^\dagger[\omega_2(k_2)]\,, \tag{3}$$

where the δ function reflects the perfect frequency phase matching and ψ is a sinc function of $\Delta k\equiv k_1+k_2-k_p$ due to the finite length of the crystal. $a_o^\dagger$ and $a_e^\dagger$ are the creation operators of the ordinary- and extraordinary-ray modes of the BBO crystal. Working in a right-handed natural coordinate system, in which the positive $\hat{z}$ direction is always the same as the $\mathbf{k}$ vectors, the field operators at the detectors are given by

$$E_1^{(+)}(t)=\alpha_t\int d\omega f(\omega)\{(\hat{\mathbf{e}}_{X1}\cdot\hat{\mathbf{e}}_{D1})\exp(-i\omega t_{f1})[(\hat{\mathbf{e}}_o\cdot\hat{\mathbf{e}}_X)a_o(\omega)+(\hat{\mathbf{e}}_e\cdot\hat{\mathbf{e}}_X)a_e(\omega)]+(\hat{\mathbf{e}}_{Y1}\cdot\hat{\mathbf{e}}_{D1})\exp(-i\omega_{t_{s1}})[(\hat{\mathbf{e}}_o\cdot\hat{\mathbf{e}}_Y)a_o(\omega)+(\hat{\mathbf{e}}_e\cdot\hat{\mathbf{e}}_Y)a_e(\omega)]\}\,, \tag{4}$$

$$E_2^{(+)}(t)=\alpha_r\int d\omega f(\omega)\{(\hat{\mathbf{e}}_{X2}\cdot\hat{\mathbf{e}}_{D2})\exp(-i\omega t_{f2})[(\hat{\mathbf{e}}_o\cdot\hat{\mathbf{e}}_X)a_o(\omega)+(\hat{\mathbf{e}}_e\cdot\hat{\mathbf{e}}_X)a_e(\omega)]+(\hat{\mathbf{e}}_{Y2}\cdot\hat{\mathbf{e}}_{D2})\exp(-i\omega t_{s2})[(\hat{\mathbf{e}}_o\cdot\hat{\mathbf{e}}_Y)a_o(\omega)+(\hat{\mathbf{e}}_e\cdot\hat{\mathbf{e}}_Y)a_e(\omega)]\}\,,$$

where $t_{fi} \equiv t - r_{fi}/c$ corresponds to the photon taking the fast optical path, of length r_{fi}, to the ith detector, which has its analyzer oriented along $\hat{\mathbf{e}}_{Di}$. An analogous definition holds for t_{si}, which corresponds to the slow optical path. $f(\omega)$ is the spectral transmission function of the filters with bandwidths σ and α_t and α_r are the complex transmission and reflection coefficients of the beam splitter. The polarization direction vectors $\hat{\mathbf{e}}_X$ and $\hat{\mathbf{e}}_Y$ correspond to the fast and slow paths through the 11 birefringent quartz plates. Likewise, $\hat{\mathbf{e}}_{Xi}$ and $\hat{\mathbf{e}}_{Yi}$ correspond to the fast and the slow paths through the ith Pockel cell.

The coincidence counting rate is therefore given by

$$R_c = (1/T)\int\int_0^T dT_1 dT_2 \langle \psi | E_1^{(-)} E_2^{(-)} E_1^{(+)} E_2^{(+)} | \psi \rangle \times S(T_2 - T_1) = (1/T)\int\int_0^T dT_1 dT_2 |\Psi(t_1,t_2)|^2 S(T_2 - T_1) , \quad (5)$$

where T_i is the detection time of the ith detector and $S(T_2 - T_1)$ is a function describing the coincidence circuit, which we approximate as one when the coincidence time window is large enough. An effective two-photon wave function that is realized by the coincidence measurements is defined in Eq. (5):

$$\Psi(t_1,t_2) = \langle 0 | E_1^{(+)}(t_1) E_2^{(+)}(t_2) | \psi \rangle . \quad (6)$$

Substituting (3) and (4) into (6), we find

$$\Psi(t_1,t_2) = \alpha_t \alpha_r \{ 2(\hat{\mathbf{e}}_{X1}\cdot\hat{\mathbf{e}}_{D1})(\hat{\mathbf{e}}_{X2}\cdot\hat{\mathbf{e}}_{D2})(\hat{\mathbf{e}}_o\cdot\hat{\mathbf{e}}_X)(\hat{\mathbf{e}}_e\cdot\hat{\mathbf{e}}_X) A(X_1,X_2) + 2(\hat{\mathbf{e}}_{Y1}\cdot\hat{\mathbf{e}}_{D1})(\hat{\mathbf{e}}_{Y2}\cdot\hat{\mathbf{e}}_{D2})(\hat{\mathbf{e}}_o\cdot\hat{\mathbf{e}}_Y)(\hat{\mathbf{e}}_e\cdot\hat{\mathbf{e}}_Y) A(Y_1,Y_2) + (\hat{\mathbf{e}}_{X1}\cdot\hat{\mathbf{e}}_{D1})(\hat{\mathbf{e}}_{Y2}\cdot\hat{\mathbf{e}}_{D2})[(\hat{\mathbf{e}}_o\cdot\hat{\mathbf{e}}_X)(\hat{\mathbf{e}}_e\cdot\hat{\mathbf{e}}_Y) + (\hat{\mathbf{e}}_e\cdot\hat{\mathbf{e}}_X)(\hat{\mathbf{e}}_o\cdot\hat{\mathbf{e}}_Y)] A(X_1,Y_2) + (\hat{\mathbf{e}}_{Y1}\cdot\hat{\mathbf{e}}_{D1})(\hat{\mathbf{e}}_{X2}\cdot\hat{\mathbf{e}}_{D2})[(\hat{\mathbf{e}}_o\cdot\hat{\mathbf{e}}_Y)(\hat{\mathbf{e}}_e\cdot\hat{\mathbf{e}}_X) + (\hat{\mathbf{e}}_e\cdot\hat{\mathbf{e}}_Y)(\hat{\mathbf{e}}_o\cdot\hat{\mathbf{e}}_X)] A(Y_1,X_2) \} . \quad (7)$$

The $A(t_1,t_2)$ are calculated as [23]

$$A(t_1,t_2) = A_0 \exp[-\sigma_p^2 (t_1+t_2)^2/8] \times \exp[-\sigma^2 (t_1 - t_2 - DL/2)^2/4] \times \exp(-i\omega_1 t_1) \exp(-i\omega_2 t_2) , \quad (8)$$

where A_0 is a normalization constant, σ_p is the pump bandwidth, and $D \equiv 1/u_0 - 1/u_e$ is a group-velocity dispersion term between the o-ray and the e-ray modes of the BBO crystal of length L. These $A(t_1,t_2)$ terms describe the four possible two-photon probability amplitudes. However, it is interesting to see that the $A(X_1,Y_2)$ and $A(Y_1,X_2)$ terms do not contribute to the coincidence counting rate as a result of the spin entanglement inherent in this type of observation of the two-photon state originating from type-II SPDC. Considering that $\hat{\mathbf{e}}_X$ is oriented at 45° relative to the o-ray plane of the BBO we see that the two scalar products inside the square brackets of the coefficient of the $A(X_1,Y_2)$ term are exactly opposite and this probability amplitude vanishes. In the same way, the coefficient of $A(Y_1,X_2)$ vanishes and the output is therefore the EPR state (2) describing the two indistinguishable processes in which both photons pass through the fast channels or both photons pass through the slow channels of the 11 quartz plates and Pockel cells.

The coincidence counting rate is therefore given by

$$R_c \sim R_0[1 - \cos(\omega_1\Delta_1 + \omega_2\Delta_2)] , \quad (9)$$

where Δ_i is the total delay between the two possible optical paths leading to the ith detector. When the optical delays introduced by the Pockel cells are increased in tandem (i.e., $\Delta_1 = \Delta_2$), Eq. (9) predicts a sinusoidal modulation at the pump frequency with 100% visibility. If the optical delay introduced by one of the Pockel cells is held fixed while the other is varied, we expect a sinusoidal modulation at the signal or idler frequency. The experimental results of these two cases are shown in Figs. 2 and 3.

In Fig. 2 the optical delays introduced by the Pockel cells were increased together by simultaneously changing the applied voltages. The coincidence counting rate data were then fitted by a sinusoidal curve with (88.2±1.2)% visibility and a period corresponding to the pump wavelength of 351.1 nm. For the data displayed in Fig. 3, Δ_2 was held fixed and Δ_1 was varied by synchronously increasing the applied voltages on the two Pockel cells that were placed in the transmission output path of the beam splitter, resulting in a period corresponding to the signal wavelength. In both cases the single detector counting rates are seen to be constant.

The quantum-mechanical predictions shown in Eq. (9) are of the type needed to demonstrate a violation of Bell's inequality based on space-time variables. As has been shown [24–26], the violation occurs whenever the visibility of the space-time interference modulation is greater

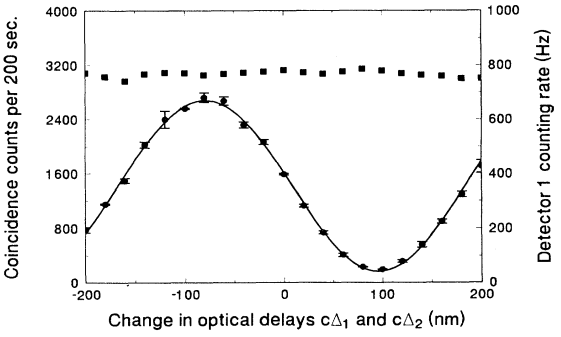

FIG. 2. Coincidence (lower part) and single detector (upper part) counting data as the delays in both output paths of the beam splitter are varied by changing the voltages on the Pockel cells. The solid line is a sinusoidal fit with period corresponding to the pump wavelength. The negative values correspond to negative voltages.

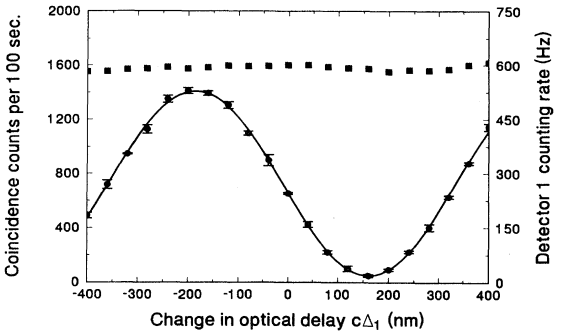

FIG. 3. Coincidence (lower part) and single detector (upper part) counting data as the delay introduced in the transmission output path of the beam splitter is varied.

than $1/\sqrt{2}=70.7\%$. We may therefore infer a violation of more than 14 standard deviations from the data presented in Fig. 2.

Furthermore, at points when the space-time interference is totally constructive or destructive, state (2) can be equivalently written in the polarization state form

$$|\psi\rangle=|X_1\rangle|X_2\rangle\pm|Y_1\rangle|Y_2\rangle\ , \tag{10}$$

where $|X_i\rangle$ and $|Y_i\rangle$ respectively correspond to the states polarized along the fast and the slow axes of the quartz plates and the ith Pockel cell. The coincidence counting rate here is seen to have a sinusoidal dependence on the difference in analyzer settings [27]. It is therefore interesting to demonstrate a violation of a Bell-type inequality based on polarization in the same experiment. Because of the symmetries present in this setup, we are able to study the inequality derived by Clauser and coworkers [4,24]

$$\delta=\left|\frac{R_c(\pi/8)-R_c(3\pi/8)}{R_0}\right|\leq\frac{1}{4}\ , \tag{11}$$

where $R_c(\phi)$ is the coincidence counting rate with the difference in analyzer settings at ϕ and R_0 is the coincidence counting rate with both analyzers removed. With the applied voltages on each Pockel cell set so that the optical path delays correspond to a minimum of the coincidence counting rate shown in Fig. 2, the analyzers were set so that the values of each of the quantities in expression (11) could be accumulated. The experimentally measured value was $\delta=0.309\pm0.009$, implying a violation of more than 6 standard deviations.

In conclusion, the counterintuitive implications of Bell's theorem warrant experimental testing of the inequalities in as many different situations as are conceivable. Whereas the first tests were based on spin observables, recent work in another direction has been done based on continuous variables. We have demonstrated here a completely different situation in which it is possible to perform tests of Bell's inequalities based on either polarization or space-time variables in a single experimental setup. This opportunity arises by taking advantage of the interesting properties of the double entangled state, which originates from type-II SPDC.

We gratefully acknowledge many useful discussions with D. N. Klyshko. This work was supported by the Office of Naval Research Grant No. N00014-91-J-1430.

[1] A. Einstein, B. Podolsky, and N. Rosen, Phys. Rev. **47**, 777 (1935).
[2] J. S. Bell, Physics **1**, 195 (1964).
[3] D. Bohm, *Quantum Mechanics* (Prentice-Hall, Englewood Cliffs, NJ, 1951), pp. 614–622.
[4] S. J. Freedman and J. F. Clauser, Phys. Rev. Lett. **28**, 938 (1972).
[5] J. F. Clauser, Phys. Rev. Lett. **36**, 1223 (1976).
[6] E. S. Fry and R. C. Thompson, Phys. Rev. Lett. **37**, 465 (1976).
[7] A. Aspect, J. Dalibard, and G. Roger, Phys. Rev. Lett. **47**, 460 (1981); **49**, 91 (1982); **49**, 1804 (1982).
[8] W. Perrie, A. J. Duncan, H. J. Beyer, and H. Kleinpoppen, Phys. Rev. Lett. **54**, 1790 (1985).
[9] C. O. Alley and Y. H. Shih, in *Proceedings of the Second International Symposium on Foundations of Quantum Mechanics in the Light of New Technology, Tokyo, 1986,* edited by M. Namiki *et al.* (Physical Society of Japan, Tokyo, 1987), p. 47; Y. H. Shih and C. O. Alley, Phys. Rev. Lett. **61**, 921 (1988).
[10] Z. Y. Ou and L. Mandel, Phys. Rev. Lett. **61**, 50 (1988).
[11] M. D. Reid and D. F. Walls, Phys. Rev. A **34**, 1260 (1986).
[12] P. Grangier, M. J. Postasek, and B. Yurke, Phys. Rev. A **38**, 3132 (1988).
[13] M. Zukowski and J. Pykacz, Phys. Lett. A **127**, 1 (1988).
[14] J. G. Rarity and P. R. Tapster, Phys. Rev. Lett. **64**, 2495 (1990).
[15] J. D. Franson, Phys. Rev. Lett. **62**, 2205 (1989).
[16] J. G. Rarity, P. R. Tapster, E. Jakeman, T. Larchuk, R. A. Campos, M. C. Teich, and B. E. A. Saleh, Phys. Rev. Lett. **65**, 1348 (1990).
[17] P. G. Kwiat, A. M. Stienberg, and R. Y. Chiao, Phys. Rev. A **47**, R2472 (1993).
[18] D. N. Klyshko, *Photons and Nonlinear Optics* (Gordon and Breach Science, New York, 1988).
[19] J. Brendel, E. Mohler, and W. Martienssen, Phys. Rev. Lett. **66**, 1142 (1991).
[20] Y. H. Shih, A V. Sergienko, and M. H. Rubin, Phys. Rev. A **47**, 1288 (1993).
[21] Y. H. Shih and A. V. Sergienko, Phys. Lett. A **191**, 201 (1994).
[22] Y. H. Shih and A. V. Sergienko, Phys. Lett. A **186**, 29 (1994).
[23] A general theory of two-photon entanglement in type-II SPDC can be found in M. H. Rubin, D. N. Klyshko, Y. H. Shih, and A. V. Sergienko, Phys. Rev. A **50**, 5122 (1994).
[24] J. F. Clauser and A. Shimony, Rep. Prog. Phys. **41**, 1881 (1970).
[25] J. F. Clauser and M. A. Horne, Phys. Rev. D **10**, 526 (1970).
[26] Z. Y. Ou, Phys. Rev. A **37**, 1607 (1988).
[27] A detailed study of the spin entanglement in a related experiment can be found in an earlier paper: T. E. Kiess, Y. H. Shih, A. V. Sergienko, and C. O. Alley, Phys. Rev. Lett. **71**, 3893 (1993).